Modeling of mass transfer during continuous drying of *Urtica urens* leaves

Haytem Moussaoui*, Ali Idlimam, Abdelkader Lamharrar, Zakaria Tagnamas, Mounir Kouhila, Younes Bahammou

Laboratory of Solar Energy and Medicinal Plants, Teacher's Training College, Cadi Ayyad University, BP 2400 Marrakesh, Morocco.

Abstract *Urtica urens* is one of the main medicinal plants used in the pharmaceutical industry and traditional medicine. It is necessary to know the process of drying and storage of this product. This work is a contribution to the understanding of the mass transfer mechanisms by modeling the drying process of the *Urtica urens* leaves. The isothermal diffusive model is based on solving the one-dimensional Fick equation. Moreover, an algorithm of minimization compiled by MATLAB is used in this study to get the optimal parameters of the model. The results showed a reasonably good agreement between the values predicted from the model and the experimental observations. This confrontation has helped to identify the diffusion coefficient and the activation energy of the *Urtica urens* leaves. The effective diffusivity values changed from 4.94 10^{-11} to 9.66 10^{-11} $m^2.s^{-1}$ within the given temperature range, and the activation energy was found to be 29.34 $kJ.mol^{-1}$. In fact, the proposed model accurately describes, on a macroscopic scale, mass transfer processes in the product.

Keywords: *Urtica urens* leaves; drying; mass transfer; effective diffusivity; modeling; Fick equation.

1. Introduction

The leaves of *Urtica urens* is a medicinal plant that is considered as an important pharmaceutical source. It has a huge value in industries that produce a large number of drugs (Gorzalczanya et al. 2011). Urtica urens is also used in traditional medicine; it is used for urinary tract infections, kidney stones, allergies, hay fever, and osteoarthritis (Marrassini et al. 2010). Therefore, drying process is essential for preserving this agricultural product. It leads to reduce the water activity in the product; hence, decreasing the rate of microbial contamination (Moussaoui et al. 2017).

* Corresponding author: Haytem.moussaoui@gmail.com   Telephone number: +212676556667

In terms of physics, the drying results from a heat and mass transfer due to the application of a heat flux on the material to be dried (Moussaoui et al. 2018a; Moussaoui et al. 2018b). The difference between the surface exposed to the flow and the drying of the product environment in terms of water concentration establishes a flow of water to the outside. This can cause a volumetric shrinkage of materials to be dried. Any drying process must take into account the specific nature and characteristics of the products, and respect certain criteria and constraints such as product quality, cost and speed of production. In this context, various scientific studies have helped develop the theory of drying. The first scientific work on drying, dating back to the 1920s by Lewis (Lewis et al. 1921) and Sherwood (Sherwood et al. 1929) provides a diffusion equation, which reflects Fick's law with a constant diffusion coefficient to describe the drying phases. A significant step was taken again, thirty years later, with the discovery by Philip and De Vries (Philip and Vries, 1957), of the role of heat transfer phenomenon in mass transfer. With the evolution of computers, several models have been developed to describe the drying phenomenon (Adibhatla and Kaushik, 2014; Ertekinb and Yaldiz, 2004; Belghit et al. 2000).

The choice of the approach is prompted by the purpose of the work undertaken, the type of the product and the internal mass transfer. In particular, there are works that are interested in identifying the diffusion coefficient by comparing the theoretical and experimental results (Zogzas et al. 1996; Boudhrioua et al. 2003).

This paper is a contribution to the understanding of mass transfer mechanisms by modeling the kinetics drying of the *Urtica urens* leaf. Additionally, the uses of the algorithm of minimization compiled by MATLAB is crucial to get the optimal parameters of the model. As a result, we get mathematical model with optimal parameters that minimize the residue between the model values and the experimental data.

2. Material and methods

2.1 Hypothesis

Due to the complexity of the phenomena, we have formulated simplified assumptions related, on the one hand, to the nature of the product and, on the other hand, to the humidity transfer mechanism within the product:

- The product's temperature and water content initial distributions are assumed spatially uniform and constant.
- The sample is an *Urtica urens* leaf.

- Transfer within the product is limited by the internal migration of moisture in liquid form, and water evaporation occurs only at the surface.
- Isothermal matrix diffusion: no direct coupling of mass transfer and heat, i.e. the transfer of material inside the product is accompanied by very fast heat transfer. Therefore, the heat exchanges corresponding to the conduction and vaporization do not generate a temperature gradient in the examined body. The model we develop is based on the Fick equation of an *Urtica urens* leaf (*Urtica urens*) of planar geometry of length (L) and thickness (e). The proposed scientific approach allows the calculation of the diffusion coefficient of *Urtica urens* leaf by the inverse method in two successive steps:
- Dynamic experimental measurement of the mass loss;
- Identification of the diffusion coefficient by minimizing the objective function defining the difference between the experimental data and the theoretical data for the dynamic drying.

2.2 Theoretical model

The sample of the plant (Fig.1) is cut in a rectangular shape (5cm×1cm); the thickness e (e = 0.05 ±0.005 mm) is very small compared to the other dimensions (length and width); the diffusion process is then one-dimensional in the direction of the sample's thickness.

The sample is immersed in an environment of constant relative humidity. Fick's equation is referred to as the one-dimensional diffusion equation (Kechaou and Maâlej, 2000). It can be solved for the spatially and temporally varying moisture content $X(x,t)$ with sufficient initial and boundary conditions (Krishna, 1993; Matuszak et al. 2005; Zamengo et al. 2017). In general, the diffusion coefficient D may vary with the local condition of turbulence; but an interesting case is, of course, that of a constant D.

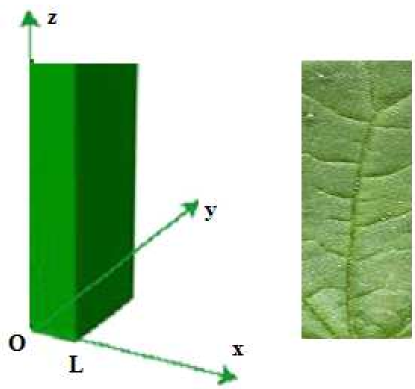

Fig. 1. Rectangular cut of *Urtica urens* leaf.

$$\frac{\partial X(x,t)}{\partial t} = D\frac{\partial^2 X(x,t)}{\partial x^2} \qquad 0<x<L \qquad t>0 \tag{1}$$

Where t is drying time, L is the thickness of the leaf and x represents the position.

Initial and boundary conditions:

$$X(x,0) = X_0 \qquad \text{At} \qquad t = 0 \tag{2}$$

$$X(0,t) = X_{eq} \qquad \text{In} \qquad x = 0 \tag{3}$$

$$X(L,t) = X_{eq} \qquad \text{In} \qquad x = L \tag{4}$$

This problem is not homogeneous because of the boundary conditions. It should be split in two problems: a stationary problem of solution $X_s(x)$ and a homogeneous problem of solution $X_h(x,t)$ (Özisik et al. 1993).

2.2.1 Stationary Problem

Under the effect of thermal agitation, there is a movement of components from areas of high concentration to those of low concentration. After some time, it can be considered as a stationary problem.

$$\frac{d^2 X_s}{dx^2} = 0 \tag{5}$$

To solve this stationary problem, we divided it into two systems of equations, according to the boundary conditions:

Firstly:

$\frac{d^2 X_{1s}}{dx^2} = 0$; the solution has the form. $\quad X_{1s} = Ax + B$

For $x = 0$; $X_{1s} = X_{eq}$ so $B = X_{eq}$

For $x = L$; $X_{1s} = 0$ so $A = -\frac{X_{eq}}{L}$

The solution is:

$$X_{1s} = -\frac{X_{eq}}{L}x + X_{eq} \tag{6}$$

Secondly:

$\frac{d^2X_{2s}}{dx^2}=0$; $X_{2s}=A'x+B'$

For $x=0$; $X_{2s}=0$ so $B'=0$

For $x=L$; $X_{1s}=X_{eq}$ so $A'=+\frac{X_{eq}}{L}$

The solution is:

$$X_{2s}=\frac{X_{eq}}{L}x \quad (7)$$

The solution of the stationary problem becomes:

$X_s=X_{1s}+X_{2s}$ therefore we find: $X_s=X_{eq}$ (8)

2.2.2 Homogeneous Problem

The particle scattering phenomenon arises from inhomogeneity concentration, and the particle stream tends to homogenize these quantities (homogeneous problem).

$$\frac{\partial X_h(x,t)}{\partial t}=D\frac{\partial^2 X_h(x,t)}{\partial x^2} \qquad 0<x<L \qquad t>0 \quad (9)$$

$X_h=0$ In $x=0$

$X_h=0$ In $x=L$

$X_h=X_0-X_s$ To $t=0$

Solution: Variable Separation Method

The function $X_h(x,t)$ can be written in the form of two separable variable functions:

$$X_h(x,t)=\Gamma(t)\psi(x) \quad (10)$$

Expression (9) becomes:

$$\frac{1}{D}\frac{\partial(\Gamma(t)\psi(x))}{\partial(t)}=\frac{\partial^2(\psi(x)\Gamma(t))}{\partial x^2} \quad (11)$$

The left side is only a function of time and the right-hand side is a function of space alone. Equality is possible if the two ratios are equal to the same constant as $-\beta^2$. Thus, we have:

$$\frac{1}{D\Gamma(t)}\frac{d\Gamma(t)}{d(t)}=\frac{1}{\psi(x)}\frac{d^2\psi(x)}{dx^2}=-\beta^2 \tag{12}$$

$$\frac{1}{D\Gamma(t)}\frac{d\Gamma(t)}{d(t)}=-\beta^2 \quad ; \quad \frac{d\Gamma(t)}{d(t)}=-\beta^2 D\Gamma(t)$$

$$\Gamma(t)=e^{-\beta^2 Dt} \tag{13}$$

The spatial function $\psi(x)$ satisfies the differential equation:

$$\frac{d^2\psi(x)}{dx^2}+\beta^2\psi(x)=0 \text{ With } \psi=0 \text{ for } x=0 \text{ and } \psi=0 \text{ for } x=L \tag{14}$$

For $\psi(x)=A_1\sin(\beta x)+A_2\cos(\beta x)$ is the solution of the above system. Therefore, the general solution of the homogeneous problem is the following (Özisik et al. 1993):

$$X_h(x,t)=\sum_{m=1}^{\infty}e^{-D\beta_m^2 t}\frac{1}{N}\psi(x,\beta_m)\int_0^L\psi(\beta_m,x')(X_0-X_s)dx' \tag{15}$$

Injecting of $\psi(x)$ in the boundary conditions (Eq. (14)) allows the determination of the coefficients A_1 et A_2

For $x=0$ we have $\psi(0)=0$ this implies that $A_2=0$

For $x=L$ we have $\psi(L)=0$, we will have $A_1\sin(\beta L)=0$; A_1 being different from zero where $\sin(\beta L)=0$ so $\beta_m=\frac{m\pi}{L}$. $\psi(x)$ is written after normalization $\psi(x,\beta_m)=\sin(\beta_m x)$

$N(\beta_m)=\int_0^L\left[\psi\left(\beta_m,x'\right)\right]^2dx'$; We show that: $N=\frac{L}{2}$

$\int_0^L\psi(\beta_m,x')(X_0-X_s)dx'=2\frac{X_0-X_s}{\beta_m}$ With m = 2n + 1, n = 0, 1, 2…∞

The homogeneous solution is: $X_h(x,t)=\sum_{m=1}^{\infty}e^{-D\beta_m^2 t}\frac{2(X_0-X_s)}{L\beta_m}(1-\cos m\pi)\sin(\beta_m x)$ (16)

The general solution of the initial problem is the sum of the stationary solution and the homogeneous solution.

$$X(x,t)=X_h(x,t)+X_{eq}$$

$$X(x,t) = X_{eq} + \sum_{m=1}^{\infty} e^{-D\beta_m^2 t} \frac{2(X_0 - X_{eq})}{L\beta_m}(1-\cos m\pi)\sin(\beta_m x) \tag{17}$$

We have then determined the moisture content $X(x,t)$ and the local relative humidity is given by:

Several authors, based on the Van Meel transformation (Van Meel, 1958), have used simply the initial moisture content X_0 and the equilibrium moisture content X_{eq} to obtain dimensionless moisture ratio $X^*(x,t)$.

$$X^*(x,t) = \frac{X(x,t) - X_{eq}}{X_0 - X_{eq}}$$

$$X^*(x,t) = \frac{2}{L}\sum_{m=1}^{\infty} \frac{e^{-D\beta_m^2 t}}{\beta_m}(1-\cos m\pi)\sin(\beta_m x) \tag{18}$$

By deriving the Eq. (18) we obtain the dimensionless drying rate.

$$f(x,t) = -\frac{\partial X^*(x,t)}{\partial t}$$

Thus:

$$f(x,t) = \frac{2D}{L}\sum_{m=1}^{\infty} \beta_m e^{-D\beta_m^2 t}(1-\cos m\pi)\sin(\beta_m x) \tag{19}$$

$X^*(x,t)$ Gives the distribution of the moisture content as a function of time in the sample. However, what relationship is there between moisture content $X^*(x,t)$ and the dimensionless mass loss $m^*(t)$?

$$m^*(t) = \frac{m(t) - m_{eq}}{m_0 - m_{eq}}$$

$m(t)$ the mass of the sample as a function of time.

$m_0 = m(t=0)$ the initial sample mass.

$m_{eq} = m(t \to \infty)$ the mass at the end of drying.

$$X(x,t) = \frac{m(x,t) - m_s}{m_s} \tag{20}$$

m_s the dry weight of the sample after complete drying at a temperature of 105 ° C .

$$X_{eq} = \frac{m_{eq} - m_s}{m_s} \tag{21}$$

$$X_0 = \frac{m_0 - m_s}{m_s} \tag{22}$$

Injection expressions $X(x,t)$, X_{eq} and X_0 in expression (Eq. (18)) give:

$$\frac{X(x,t) - X_{eq}}{X_0 - X_{eq}} = \frac{m(x,t) - m_{eq}}{m_0 - m_{eq}} \tag{23}$$

So, $X^*(x,t) = m^*(x,t)$

$$m^*(x,t) = \frac{m(x,t) - m_{eq}}{m_0 - m_{eq}}$$

However, the mass is an overall measure of the sample that does not depend on the position. Therefore, the answer is that the mass $m^*(t)$ is the average, over the sample $X^*(x,t)$ i.e.:

$$\overline{X}^*(t) = \frac{1}{L}\int_0^L X^*(x,t)dx$$

$$\overline{X}^*(t) = \sum_{m=1}^{\infty} \frac{2}{L^2 \beta_m^2}(1 - \cos m\pi)^2 e^{-D\beta_m{}^2 t} \tag{24}$$

The dimensionless drying rate f is given by:

$$f = \left|\frac{dX^*}{dt}\right| \quad \text{So} \quad f = \left|\frac{dm^*}{dt}\right|$$

$$f(t) = -D\sum_{m=1}^{\infty} \frac{2}{L^2}(1 - \cos m\pi)^2 e^{-D\beta_m{}^2 t} \tag{25}$$

The outcomes are the two models expressed in Eq. (24) and Eq. (25); they present the relationship between the moisture ratio and the drying time, as well as the dimensionless drying rate in function of drying time respectively.

2.3 Algorithm minimization

"Optimization Toolbox" extends the MATLAB technical computing environment with tools and widely used algorithms for standard optimization. These algorithms solve continuous and discrete problems with and without constraints. The toolbox includes functions for linear programming, quadratic programming, nonlinear optimization, nonlinear least squares, nonlinear equations, optimizing several objectives and binary integer programming.

MATLAB and "Optimization Toolbox" toolbox allow easily defining models, gathering data, managing model formulations, and analyzing results. They offer engineers and scientists the tools needed to find optimal solutions, analyze the various compromises, balance different design options and quickly incorporate optimization methods in their algorithms and models.

The functions of the toolbox, accessed via the MATLAB command line, are written in the open MATLAB language. This means that you can inspect the algorithms, modify the source code and create your own custom functions.

The "Optimization Toolbox" contains the most widely used minimizing and maximizing methods. This toolkit implements standard algorithms at a large scale, so you can take advantage of problems with hollow or structure. The command line interface allows you to access the tools to define, execute and evaluate the optimization (Table 1). You can also manipulate and diagnose your optimization using the diagnostic outputs from the optimization methods.

Using an output function, you can also write the results to files, create your own stopping criteria, and write your own graphical interfaces to run the solvers of the toolbox.

lsqcurvefit solves the adjustment curve of non-linear precision (data-fitting) problems in the least squares sense. The input data is inputted (xdata), and the output data is observed (ydata), find the coefficient X of the equation "best-fit".

$$\min_x \frac{1}{2}\left\| F(param, xdata) - ydata \right\|^2 = \frac{1}{2}\sum_i \left(F(param, xdata_i) - ydata_i\right)^2$$

Where xdata and ydata are vectors and F (x, xdata) is a function evaluated by a vector.

$$\min_x \frac{1}{2}\left\| \overline{\overset{*}{X}}(D,t) - m^*{}_{\exp}(t) \right\|^2 = \frac{1}{2}\sum_{i=1}^{i=n}\left[m^*(D,t_i) - m^*{}_{\exp}(t_i) \right]^2$$

command line: [x,resnorm,residual] = ***lsqcurvefit***(fun,x0,xdata,ydata,lb,ub,options,P_1,P_2,...)

In entry:

- x_0 the vector contains the supposed value of the diffusion coefficient D: $x_0 = (D_0)$
- the xdata vector contains the time variable $xdata = (t_0, t_1, t_2, \ldots\ldots\ldots t_n)$
- the ydata vector contains the mass measured $m(t) = (m_0, m_1, m_2, \ldots\ldots\ldots m_n)$

Output:

- The vector x contains the value of the diffusion coefficient D .
- resnorm contains the value of χ^2
- residual contains difference vector $m^*(t_i) - m^*_{\exp}(t_i)$

Table 1. Minimization algorithm

Routine	Function
MinimFick.m	main Routine. • Load vectors x_0, xdata et ydata. • Call lsqcurvefit $\Rightarrow x = (D)$ • Call mafun.m $\Rightarrow$ $m^*(x, t_i)$
MafunFick.ma	mathematical model
Series	Calculation serie $m^*(t) = \sum_{m=1}^{\infty} \frac{2}{L^2 \beta_m^2} (1 - \cos m\pi)^2 e^{-D\beta_m^2 t}$
Drying Rate	Calculating the rate of drying $f = \left\| \frac{dm^*}{dt} \right\|$ $f(t) = -D \sum_{m=1}^{\infty} \frac{2}{L^2} (1 - \cos m\pi)^2 e^{-D\beta_m^2 t}$

Minimization procedure:

1) position the workspace in the directory Fick Flux
2) run minimik.m

2.4 Experimental procedure

Dehydration of a sample: dynamic measurement of mass loss, the procedure consists of:

1. adjustable temperature oven
2. an electronic precision balance ($\pm 10^{-4}$ g), and the error in the measurement of time is (± 1 s)

3. a computer
4. acquisition software Matlab data

Fig. 2.a Photo of experimental equipment

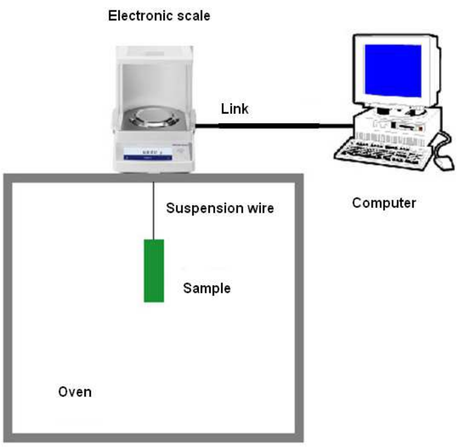

Fig. 2.b Schematic of the experimental setup

To perform the continuous drying operations, the leaf of *Urtica urens* to be dried is cut in rectangular form (5cm x 1cm). To ensure greater stability of the drying conditions and a homogenization of the temperature within the oven, it must be driven at least half an hour prior to introducing the sample (Fig. 2). The sample thickness is measured in micrometers. The sample is placed in a support to avoid deformation and change in geometry due to drying (Zlatanovi et al. 2013). We fix the five minutes´ step of no mass loss acquisition; and when that weight loss is not significant, the measurements are stopped.

3. Results and discussion

3.1 Experimental result

The experiments were conducted at temperatures 40, 50 and 60 ºC; in Fig. 3 we present three curves showing the evolution time of the moisture ratio of the product at three temperatures; and in Fig. 4, we plotted the variation of the drying rate depending on the moisture ratio (Ben Mabrouk et al. 2006; Torres et al. 2013).

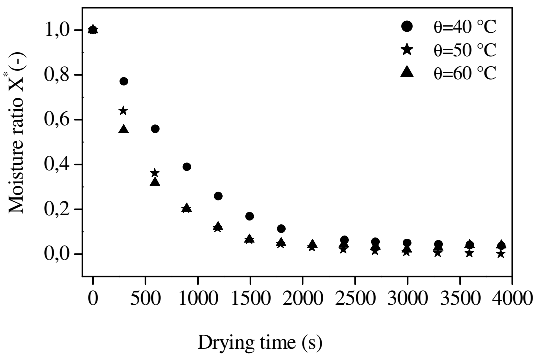

Fig. 3. Variation of moisture ratio as a function of time of *Urtica urens* leaf.

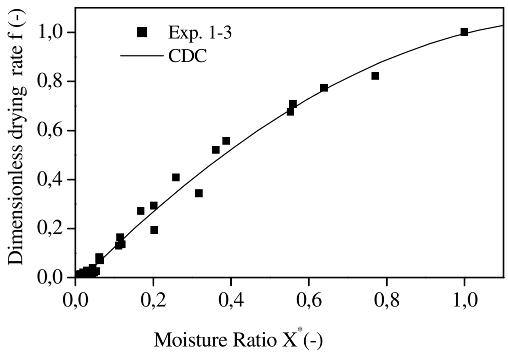

Fig. 4. Characteristic drying curve (CDC) of *Urtica urens* leaf.

3.2 Validation of the model

Table 2 shows the set of experimental values and those predicted by the theoretical model for the different temperatures.

Table 2. Moisture ratios obtained experimentally and by the mathematical model at 40, 50 and 60 ºC.

θ=40°C			θ=50°C			θ=60°C		
t(s)	$X^*_{exp}(t)$	$X^*_{pré}(t)$	t(s)	$X^*_{exp}(t)$	$X^*_{pré}(t)$	t(s)	$X^*_{exp}(t)$	$X^*_{pré}(t)$
0	1	0.9998	0	1	0.9997	0	1	0.9997
295	0.7710	0.6470	289	0.6397	0.5381	293	0.5532	0.5256
595	0.5598	0.4991	589	0.3617	0.3488	593	0.3183	0.3351
895	0.3887	0.3897	889	0.2021	0.2270	893	0.203	0.2143
1195	0.2589	0.3047	1189	0.1156	0.1477	1193	0.1206	0.137
1495	0.1686	0.2384			0.0960	1493	0.0647	0.0876
1795	0.1126	0.1865	1789	0.0454	0.0625	1793	0.0496	0.0561

2398	0.063	0.0892	2089	0.0305	0.0407	2093	0.0408	0.0359
2695	0.0547	0.0698	2389	0.0213	0.0265	2393	0.0434	0.0229
2995	0.049	0.0546	2689	0.0135	0.0172	2693	0.0328	0.0147
3295	0.0433	0.0427	2989	0.0092	0.0112	2993	0.0204	0.0094
3595	0.0401	0.0334	3289	0.0043	0.0073	3293	0.0293	0.006
3895	0.0363	0.0261	3589	0.0035	0.0047	3593	0.0399	0.0038
4195	0.0331	0.0204	3889	0.0007	0.0031	3893	0.039	0.0025
4495	0.0299	0.0160	4189	0.0001	0.0020	4193	0.0417	0.0016
4795	0.0286	0.0125	4489	0.0002	0.0013	4493	0.0204	0.001
5095	0.0254	0.0098	4789	0.0001	0.0009	4793	0.0434	0.0008
5395	0.0229	0.0077	5089	0.0043	0.0006	5093	0.0363	0.0007
5695	0.0235	0.0060	5389	0.0028	0.0004	5393	0.0301	0.0005
5995	0.0229	0.0047	5689	0.0035	0.0002	5693	0.0186	0.0001
6295	0.0223	0.0037	5989	0.005	0 .0002	5993	0.0177	0 .0002
6595	0.0223	0.0029	6289	0.0057	0.0001	6593	0.0151	0.0001

Examples of the good quality of this identification: we have shown in Fig. 5 and Fig. 6. The curves showing the evolution over time of moisture ratio and the drying rate of drying of the product predicted by the model and those determined experimentally. The good agreement between the experimental points and the theoretical ones calculated by the model seems to us adequate to stop the calculation. The minimization process determines the diffusion coefficient *D* of the plant.

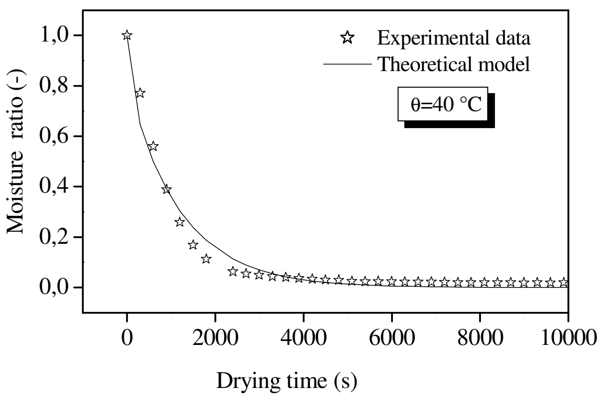

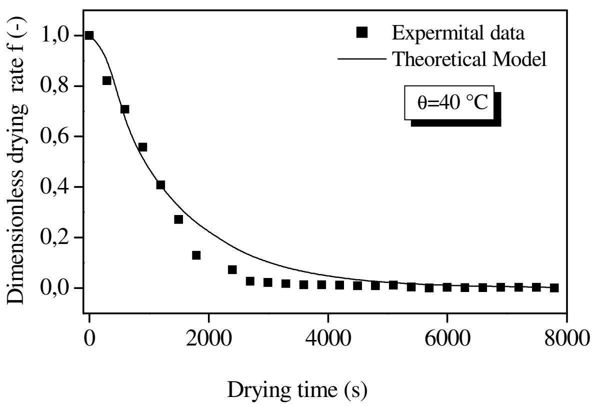

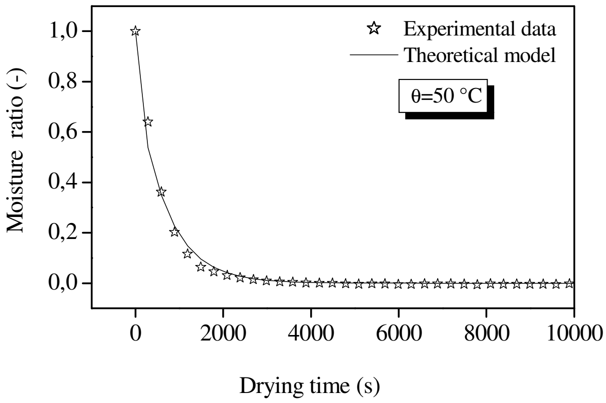

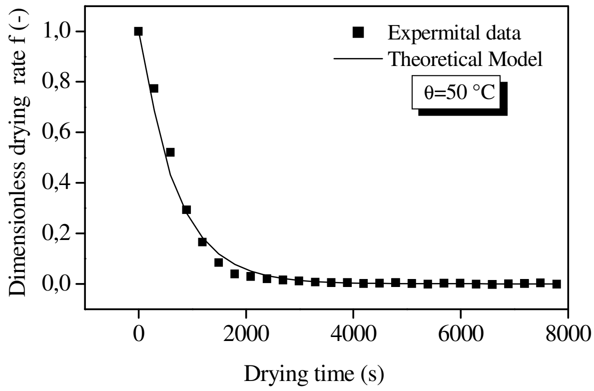

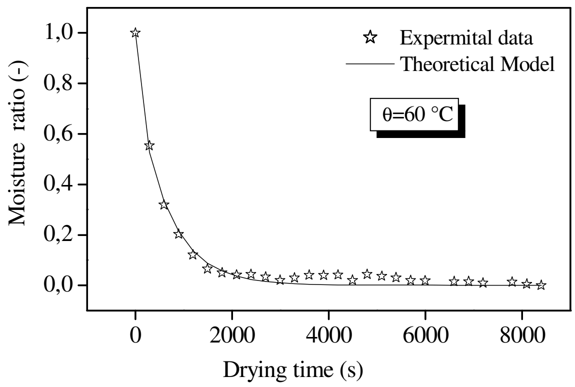

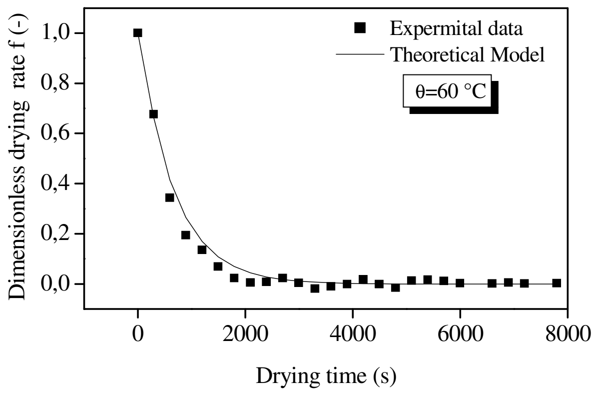

Fig. 5. Comparison between an experimental moisture ratio and calculated by Theoretical model.

Fig. 6. Comparison between an experimental dimensionless drying rate and calculated by Theoretical model.

3.3 Diffusion coefficient and activation energy

The diffusion coefficient described for *Urtica urens* leaf depending on the temperature is valid for the temperature ranging between 40, 50 and 60° C. Table 3 shows the variation of the diffusion coefficients as a function of temperature.

Table 3. Diffusion coefficients and reduced chi-square at 40, 50 and 60 °C

Temperature θ (°C)	Diffusion coefficient *D* (m^2/s)	χ^2
40	$4.94\ 10^{-11}$	0.0620
50	$9.28\ 10^{-11}$	0.0148
60	$9.66\ 10^{-11}$	0.0134

The correlation between the drying conditions and the determined values of the effective diffusivity can be expressed by using an Arrhenius type equation (Vagenas and Marinos-Kouris, 1991; Kara and Doymaz, 2015; Bezera et al. 2015) such as:

$$D = D_0 \exp\left(-\frac{E_a}{RT} \right) \tag{26}$$

Where D_0 is the pre-exponential factor of the Arrhenius equation ($m^2.s^{-1}$); E_a is the activation energy of the moisture diffusion ($kJ.mol^{-1}$); T is the air absolute temperature and R is the universal gas constant ($J.mol^{-1}.K^{-1}$).

The activation energy (E_a) was calculated from the slope of the plot of $Ln\ (D)$ against the inverse of absolute temperature (T) as shown in Fig. 7. The activation energy was found equal to 29.34 kJ mol $^{-1}$.

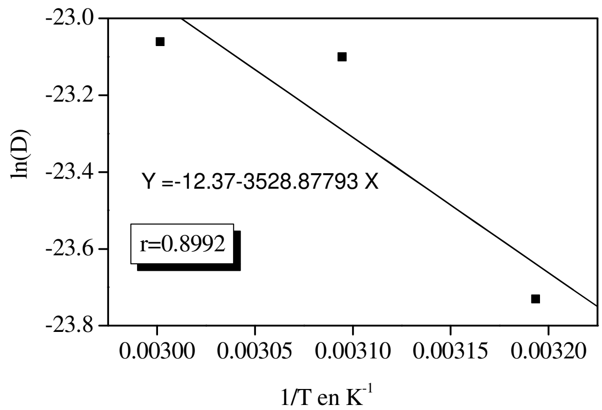

Fig. 7. Influence of drying air temperature on the effective diffusivity

4. Conclusion

In this paper, the curves are plotted over time of the reduced water content and the standardized drying rate of the product predicted by the model and those experimentally determined. The model reflects a macroscopic approach to the problem. The choice of testing strategy is guided by the expected purpose of this work. The isothermal diffusive model is based on solving the one-dimensional Fick equation. The experiment and theory confrontation concluded that overall drying kinetics of *Urtica urens* leaves provided by this theoretical model is considered perfect. This proposed scientific approach has allowed us to identify the diffusion coefficient of the product by minimizing the objective function defining the difference between the experimental data and the mathematical model of dynamic drying.

The effective diffusivity values changed from 4.94 10^{-11} to 9.66 10^{-11} $m^2.s^{-1}$ within the given temperature range and increased with increasing temperature. An Arrhenius relation with an activation energy value of 29.34 $kJ.mol^{-1}$ expressed the effect of temperature on the effective diffusivity.

Nomenclature

CDC	Characteristic drying curve
D	Diffusion coefficient ($m^2.s^{-1}$)
E_a	Activation energy ($kJ.mol^{-1}$)
f	Dimensionless drying rate (-)
L	Thickness (m)
X	Moisture content (% d.b)
X^*	Moisture ratio(-)
r	Correlation coefficient
R	Universal gas constant (8.3145 $J.mol^{-1}.K^{-1}$)
t	Drying time (s)
T	Absolute temperature (K)

Greeks

θ	Temperature (°C)
χ^2	reduced chi-square

Acknowledgments: Special thanks to the Ministry of Higher Education, Scientific Research and professional Training of Morocco, Priority Research Program (PPR-B-Mahrouz- FS-UCA-Marrakesh).

References

Adibhatla, S. and Kaushik, S.C., 2014. Energy and exergy analysis of a super critical thermal power plant at various load conditions under constant and pure sliding pressure operation, App. *Thermal Eng.,* vol. 73, pp. 49-63. doi.org/10.1016/j.applthermaleng.2014.07.030

Belghit, A. Kouhila, M. and Boutaleb, B-C., 2000. Experimental study of drying kinetics by forced convection of aromatic plants, *Ener. Conver. Manag.,* vol. 41, no. 12, pp. 1303-1321. doi.org/10.1016/s0196-8904(99)00162-4

Boudhrioua, N. Bonazzi, C. and Daudin, J-D., 2003. Estimation of moisture diffusivity in gelatin–starch gels using time-dependent concentration–distance curves at constant temperature, *Food Chem.,* Vol. 82, no .1, pp. 139-149, doi.org/10.1016/s0308-8146(02)00542-3

Ben Mabrouk, S. Khiari, B. and Sassi, M., 2006. modelling of heat and mass transfer in a tunnel dryer, *Appl. Thermal Eng.,* vol. 26, pp. 2110–2118. doi.org/10.1016/j.applthermaleng.2006.04.007

Bezera, C-V. Da Silva, M. Corrêa, D-F. and Rodrigues, A-M-C., 2015. A modelling study for moisture diffusivities and moisture transfer coefficient in drying of passion fruit peel, *Int. J. Heat. Mass. Transf.*, vol. 85, pp. 750-755, Doi.org/10.1016/j.ijheatmasstransfer.2015.02.027

Droštinová, L. Braniša, J. Bončíková, D. and Jomová, K., 2015. Effect of Drying methods in content of some natural pigment in Urtica dioica L. and Mellissa officinalis L., *Microbiol. Biotech Food Sci.,* vol. 5, no. 2, pp. 182-185. doi.org/10.15414/jmbfs.2015.5.2.182-185

Ertekin, C. and Yaldiz, O., 2004. Drying of eggplant and selection of a suitable thin layer drying model, *J. Food Eng.,* vol. 63, no. 3, pp. 349–359, doi.org/10.1016/j.jfoodeng.2003.08.007

Gorzalczanya, S. Marrassini, C. Miño, J. Acevedoa, C. and Ferraro, G., 2011. Antinociceptive activity of ethanolic extract and isolated compounds of Urtica circularis, *Ethnopharmacology*, vol. 134, no. 3, pp. 733-738, doi.org/10.1016/j.jep.2011.01.025

Krishna, R., 1993. Problems and pitfalls in the use of the fick formulation for intraparticle diffusion, Chem. Eng. Sci., vol 48, no. 5, pp. 845-861.

Moussaoui, H., Lamsyehe, H., Idlimam, A., Lamharrar, A., & Kouhila, M., 2018a. Experimental Study of the Impact of Drying Parameters on Dandelion Root by a Solar Dryer. In International Conference on Advanced Intelligent Systems for Sustainable Development (pp. 12-20). Springer, Cham.

Moussaoui, H., Idlimam, A., & Lamharrar, A., 2018b. The Characterization and Modeling Kinetics for Drying of Taraxacum Officinale Leaves in a Thin Layer with a Convective Solar Dryer. In International Conference on Electronic Engineering and Renewable Energy (pp. 656-663). Springer, Singapore.

Moussaoui, H., Aghzzaf, A. A., Idlimam, A., & Lamharrar, A., 2017. Modeling of a Forced Convection Solar Drying System by Experimental Designs. In Euro-Mediterranean Conference

for Environmental Integration (pp. 1497-1499). Springer, Cham. https://doi.org/10.1007/978-3-319-70548-4_436

Özisik, M-N., 1993. *Heat Conduction*, 2nd ed., John Wiley & Sons, New York.

Philip, J-R. and De Vries, D-A., 1957. Moisture movements in porous materials under temperature gradients, *Trans. Amer. Geoph. Union.,* vol. 38, no. 2, pp. 222-232, doi.org/10.1029/tr038i002p00222

Sherwood, T.K., 1929. The drying of solid, *Ind.Eng. Chem.,* vol. 21, no. 10, pp. 12-16, Doi.org/10.1021/ie50229a004

Torres, S.S, Jomaa, W., Puiggali, J.R., Avramidis, S., 2013. Multiphysics modeling of vacuum drying of wood, *Appl. Math. Modell.,* vol 49, pp. 31-40.

Vagenas, G.K., Marinos-Kouris, D., 1991. Finite element simulation of drying of agricultural products with volumetric changes, *Appl. Math. Modell.,* vol. 15, pp. 475-482.

Van Meel, D-A., 1958. Adiabatic convection batch drying with recirculation of air, *Chem. Eng. Sci.,* vol. 9, no. 1, pp. 36-44. doi.org/10.1016/0009-2509(58)87005-0

Zlatanovi, I. Komatina, M. and Antonijevi, D., 2013. Experimental Investigation of the Efficiency of Heat Pump Drying System with Full Air Recirculation, *App. Therm. Eng.,* vol. 53, pp. 114-123. doi.org/10.1111/jfpe.12386

Zogzas, N-P. Maroulis, N-B. and Marinoskouris, D., 1996. Moisture diffusivity data compilation in foodstuffs, *Drying Techno.,* vol. 14, no. 10, pp. 2225-2253. doi.org/10.1080/07373939608917205

Zamengo, M. Funada, T. and Morikawa, J., 2017. Thermal diffusivity measurement of erythritol and numerical analysis of heat storage performance on a fin-type heat exchanger, *Appl. Thermal Eng.,* vol. 117, pp. 376-384. doi.org/10.1016/j.applthermaleng.2017.02.040

Arabian Journal of Medicinal and Aromatic Plants

www.ajmap.info **ISSN 2458-5920**